JOURNAL OF GEOPHYSICAL RESEARCH: ATMOSPHERES, VOL. 118, 9093–9104, doi:10.1002/jgrd.50634, 2013

Impacts of woody plant encroachment on regional climate in the southern Great Plains of the United States

Jianjun Ge[1] and Chris Zou[2]

Received 1 February 2013; revised 5 July 2013; accepted 8 July 2013; published 20 August 2013.

[1] Vegetation change can influence climate by altering the fluxes of mass and energy between ecosystems and the atmosphere. In the past century or so, rapid conversion of grasslands to woodland by woody species encroachment is one of the most important vegetation changes in the semiarid and arid regions of the world. The objective of this study is to investigate potential impacts of this widespread phenomenon on climate system in the southern Great Plains of the United States. The Regional Atmospheric Modeling System (RAMS) is used for this study. Grassland on the surface in RAMS is gradually replaced by woody species and RAMS is run a set of times, each with a different amount of encroachment. RAMS-simulated precipitation and air temperature are then analyzed. This study finds tha t over a 1 year period woody plant encroachment leads to increase in rainfall and the increase is statistically significant at many locations. Woody encroachment also has an overall warming effect, but increase in temperature is not statistically significant. Temperature and precipitation increase almost linearly with increasing encroachment on the surface. When grassland is completely replaced, annual accumulated precipitation increases by 23.6 mm and maximum air temperature rises by 0.13°C averaged over the entire study area. In areas where encroachment occurs, averaged increases in accumulated precipitation and temperature are 58.2 mm and 0.27°C, respectively. The largest increase in precipitation and strongest warming tend to be located in dry and encroached areas including central and northern Texas, and they reach as high as 213.6 mm and 0.68°C, respectively. Decrease in surface albedo is found to be the most important factor that causes these changes.

Citation: Ge, J., and C. Zou (2013), Impacts of woody plant encroachment on regional climate in the southern Great Plains of the United States, *J. Geophys. Res. Atmos.*, *118*, 9093–9104, doi:10.1002/jgrd.50634.

1. Introduction

[2] Current climate models are weak at accurately simulating certain processes and associated feedbacks in the coupled atmosphere-ocean-vegetation system. An increasing number of studies suggest that the biosphere exerts considerable control over the physical systems in the atmosphere and the ocean [e.g., *Pitman et al*., 2004; *Feddema et al*., 2005; *Cotton and Pielke*, 2007; *Fall et al*., 2009; *de Noblet-Ducoudré et al*., 2011; *Pielke et al*., 2011]. So far, however, our understanding of the interaction between climate and vegetation is still limited [*Pielke et al*., 2011].

[3] Vegetation change, as a direct result of human land use activities and as a consequence of climate change, affects climate through forcing and feedback processes [*Betts*, 2006]. Large-scale changes in vegetation cover can provide sources or sinks of carbon dioxide and can affect the concentration of mineral dust aerosol particles [*Forster et al*., 2007]. Vegetation also influences climate through the surface fluxes of radiation, heat, moisture, and momentum [*Gao et al*., 2003; *Foley et al*., 2003; *Pielke et al*., 2007; *Anav et al*., 2010]. The nature of vegetation cover exerts a strong influence on the albedo of the land surface [e.g., *Nair et al*., 2007]. Relative to bare soil, vegetation can increase the evaporative flux of moisture to the atmosphere by contributing transpiration as well as surface evaporation. The higher aerodynamic roughness of a vegetated land surface also can promote the flux of moisture to the atmosphere through enhanced turbulence. Furthermore, the vegetation canopy can capture a fraction of precipitation, which is then reevaporated back to the atmosphere without infiltrating into the soil. Perhaps the best known example of vegetation impacts on climate is tropical deforestation. Model results suggest that tropical forests exert a cooling effect on their regional climates due to a plentiful supply of soil moisture and strong evapotranspiration. According to most climate modeling studies, large-scale deforestation of tropical forests will cause a considerable increase in surface temperature and a decrease in annual rainfall [e.g., *Shukla et al*., 1990].

[1]Department of Geography, Oklahoma State University, Stillwater, OK, USA.
[2]Department of Natural Resource Ecology and Management, Oklahoma State University of Agriculture and Applied Science, Stillwater, OK, USA.

Corresponding author: J. Ge, Department of Geography, Oklahoma State University, 337 Murray Hall, Stillwater, OK 74078, USA. (jianjun.ge@okstate.edu)

2169-897X/13/10.1002/jgrd.50634

Figure 1. An early-stage red cedar invasion in Oklahoma. (left) Photograph taken in summer of 2008 and (right) photograph taken in winter of 2008. Both photographs are in true color.

On the other hand, forests in cold regions exert a warming influence through their large impact on surface albedo, which outweighs the influence of transpiration [*Bonan et al*., 1992; *Betts*, 2000].

[4] One of the important vegetation changes of the past century has been conversion of the world's grasslands and savannas to woodland by woody species encroachment [*Archer*, 1994]. This phenomenon has been particularly rapid across arid and semiarid ecosystems, which cover roughly 45% of the global land surface [*Archer*, 2002; *Defries and Townshend*, 1995]. In the more mesic prairies of the eastern Great Plains, grasslands are rapidly transitioning to woodland by encroachment of eastern red cedar (*Juniperus virginiana* L. var. *virginiana*) [*Schmidt and Leatherberry*, 1995; *Fuhlendorf*, 1999; *Briggs et al*., 2002; *Engle et al*., 2007]. In northwestern Oklahoma, based on the observed rate of eastern red cedar expansion from 1965 to 1995, woody cover is projected to increase 500% by 2015 under no-control scenarios, with eastern red cedar dominating approximately 20% of the average landscape [*Coppedge et al*., 2004]. In *Coppedge et al*. [2004], the rate of woody expansion was found to be site specific and ranged from 15% to 35% in about 15 years. Texas, Kansas, and other Great Plain states are experiencing a similar encroachment. Invasion of this species is easily prevented with prescribed fire, but application of fire by livestock managers must overcome limitations in fuel associated with continuous grazing pressure and drought [*Fuhlendorf et al*., 2008] as well as landowner acceptance and ability to use fire [*Taylor*, 2005]. Also, prescribed fire may be limited by concerns about carbon loss, air quality impairment, and altered water cycles. In addition, it takes less than 10 years for a treated site to be reinfested [*Fuhlendorf et al*., 2008]. Therefore, eastern red cedar encroachment will likely be a dominant component of Great Plains rangelands far into the future. Figure 1 shows an early-stage red cedar invasion in a prairie in Oklahoma (36°03′N, 97°13′W). One photograph was taken in summer (August 2008), and the other was taken in winter (December 2008).

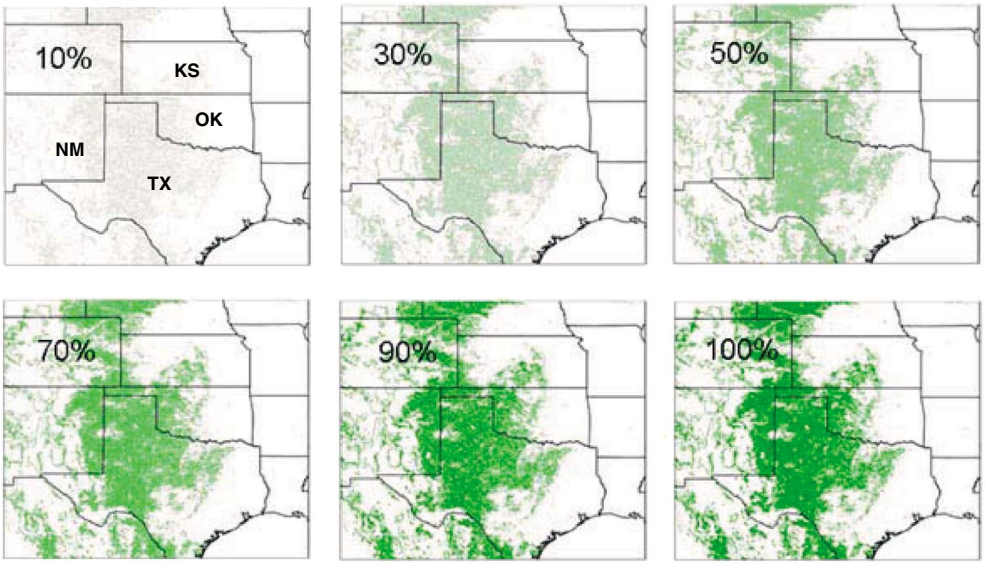

Figure 2. Study area and scenarios of woody plants expansion in grassland (selected maps only). Woody encroachment is represented by the number of the pixels. The remaining grassland as well as other land cover types are not shown for clarity.

Table 1. Major Biophysical Parameters of Vegetation in RAMS

Biophysical Parameters	Direct Effects
Albedo	Solar radiation
Leaf area index	Evaporation, transpiration, rainfall interception, etc.
Fractional vegetation cover	Ground evaporation, soil moisture, surface albedo, etc.
Root depth	Extraction of soil water and transpiration
Surface roughness	Vertical motion and turbulent fluxes

[5] Woody plant encroachment has been attributed to changes in atmospheric boundary conditions (e.g., CO_2 concentration, air temperature, precipitation) acting alone or in concert with land use changes (e.g., domestic livestock introduction, fire suppression) [*Archer et al*., 1995].The debate on the causal mechanism for this phenomenon continues, while considerably less is known about the consequences of this change on energy and water budgets at regional and global scales [*Huxman et al*., 2005; *Scott et al*., 2006].

[6] The objective of this research is to investigate potential impacts of woody plant encroachment on regional climate with a focus on the southern Great Plains of the United States. The encroachment process is generated by gradually replacing grassland with woodland in a land cover data set. A regional climate model is then run a number of times with modified land cover information. All other conditions and parameters are kept the same in the model. Model-simulated temperature and precipitation are examined to determine the impacts resulting from woody encroachment. Here, "regional climate model" means a limited area model with high resolution, generally with grid spacing less than 100 km, run for a simulation time of more than approximately 2 weeks' length, so that the initial atmospheric conditions have been forgotten [*Jacob and Podzun*, 1997; *Giorgi and Mearns*, 1999].

2. Methodology

2.1. Study Area

[7] Figure 2 shows the study area of this research. It is an area of 1800 × 1800 km and primarily covers eight states of the United States and a small area in Mexico and the Gulf of Mexico. Based on the Global Land Cover Characterization database [*Loveland et al*., 2000] developed by the U.S. Geological Survey (USGS), the land surface of the study area is dominated by six land cover types: shortgrass (25.0%), crops (22.8%), semidesert (15.7%), evergreen needleleaf forest (8.5%), deciduous broadleaf forest (8.0%), and wooded grassland (6.5%). In this study, the USGS Global Land Cover Characterization database is the land cover data set used for woody encroachment generation. It is also the default land cover data set in the climate model used in this study. This data set is based on 1 km advanced very high resolution radiometer (AVHRR) data spanning April 1992 through March 1993, and it is currently archived at the Earth Resources Observation and Science Data Center.

2.2. Regional Atmospheric Modeling System

[8] The regional climate model used for the numerical simulations in this work was the Regional Atmospheric Modeling System (RAMS) Version 4.4 [*Pielke et al*., 1992; *Cotton et al*., 2003]. The soil-vegetation-atmosphere transfer scheme employed in RAMS is the Land Ecosystem-Atmosphere Feedback model, version 2 (LEAF-2) [*Lee*, 1992; *Walko et al*., 2000]. LEAF-2 represents the storage and vertical exchange of water and energy in multiple soil layers, temporary surface water or snow cover, and vegetation and canopy air. The special feature of LEAF-2 is its ability to represent fine-scale surface variations by dividing surface grid cells into subgrid patches, which are assigned based on the land cover types in a model grid cell. Each patch has one land cover type and responds to and influences the overlying atmosphere in its own unique way according to its fractional area of coverage. The biophysical characteristics, such as albedo, leaf area index, fractional vegetation cover, etc., are then defined for the land cover type each patch possesses. In the experiments presented here, the number of patches per grid cell was set to 10 for a relatively detailed representation of the land surface. One patch is allocated for water in all grid cells.

[9] The soil model in LEAF-2 consisted of 11 vertical layers spanning a depth of 2.1 m, and the soil temperature profile was initialized based on the initial air temperature in the lowest atmospheric level. The soil moisture content for the top layer was initialized as 35% of the saturation value, which was horizontally homogeneous over the domain. This percentage was increased with depth to a maximum of 55% at 48 cm and below. Moisture flux between soil layers was parameterized in LEAF-2 based on a multilayer soil model described by *Tremback and Kessler* [1985]. Both energy and moisture fluxes between LEAF-2 components (i.e., vegetation, canopy air, and each soil and snow cover layer) are illustrated in detail by *Walko et al*. [2000].

[10] A single grid with a 1800 × 1800 km area is used as the model domain of the experiments, which covers eight states in the U.S. and small sections of surrounding states, Mexico, and the Gulf of Mexico (Figure 2). The horizontal grid spacing is set at 50 km in consideration of the domain size and the computational requirements. For the land surface, the standard RAMS 30 arc sec topography data set was used. The grid extended over 32 vertical levels, with a layer thickness of 80 m near the surface and stretching to 1900 m at the top of the domain. The model was driven by 6-hourly lateral boundary conditions derived from the National Centers for Environmental Prediction atmospheric reanalysis product [*Kalnay et al*., 1996]. The model time step

Table 2. Biophysical Parameters for Two Land Cover Classes in RAMS[a]

	Shortgrass	Wooded Grassland
Albedo	0.26	0.18
LAI	2.0	5.0
D LAI	1.5	4.0
VFC	0.8	0.8
D VFC	0.1	0.2
Roughness length	0.02	0.51
Root depth	1.0	1.0

[a]LAI and VFC are maximum leaf area index and vegetation fractional cover, respectively; D LAI and D VFC are maximum decrease in leaf area index and vegetation fractional cover, respectively. These parameters and cosine functions in temperature are utilized for simplified vegetation seasonality.

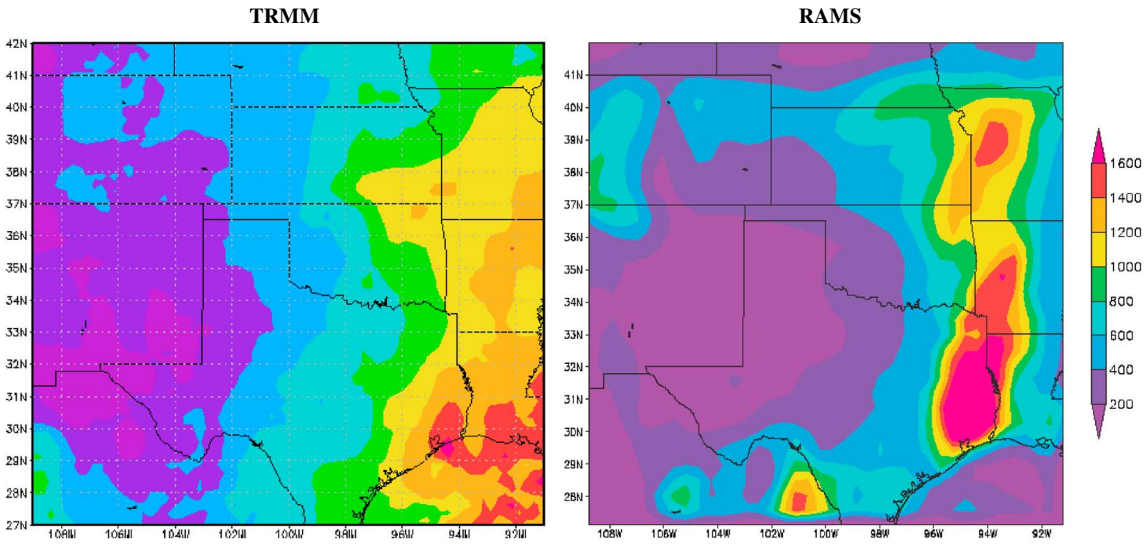

Figure 3. Comparison of accumulated precipitation (mm/yr) from observation (TRMM) and that from RAMS in the year 2003.

was 90 s with the output period set to every 3 h. At each time step, the reanalysis data were nudged over five outer grid points. The year 2003 is chosen for simulation; 2003 is a relatively normal year in terms of total precipitation. Three months in 2002 (October to December) are used as model spin-up time and are omitted in the analysis. More descriptions of the land surface scheme and other settings in RAMS can be found in *Ge et al*. [2007, 2008].

2.3. Woody Encroachment Generation

[11] The woody encroachment process has been generated by gradually replacing grassland (shortgrass) pixels with wooded grassland (red cedar) pixels in the 1 km land cover map. Figure 2 shows the generated woody plant encroachment scenarios in this region at 1 km grid increment, and these scenarios are used for climate simulation. Specifically, shortgrass pixels in the land cover map are randomly selected, and their pixel values are changed to those representing wooded grassland. The number of changed pixels increases from 0% to 100% of the original total shortgrass pixels at an interval of 10%. Figure 2 (bottom right) shows that the original grassland has been completely replaced by red cedar (green pixels). The other five panels show 10%, 30%, 50%, 70%, and 90% replacement of grassland. For clarity, the remaining grassland pixels are not shown. Other maps (0%, 20%, 40%, 60%, and 80% encroachment) are not shown in Figure 2.

[12] We recognize that the actual woody plant expansion will not occur in this random manner. Often, the expansion occurs at the best sites first but in some instances can only continue to expand under optimal conditions (i.e., edaphic, plant-plant competition, climate). Expansion can occur at a geometric rate because the expanding tree canopy cover produces a massive seed rain [e.g., *Miller and Rose*, 1995]. Still, this method is a simple and appropriate approach for

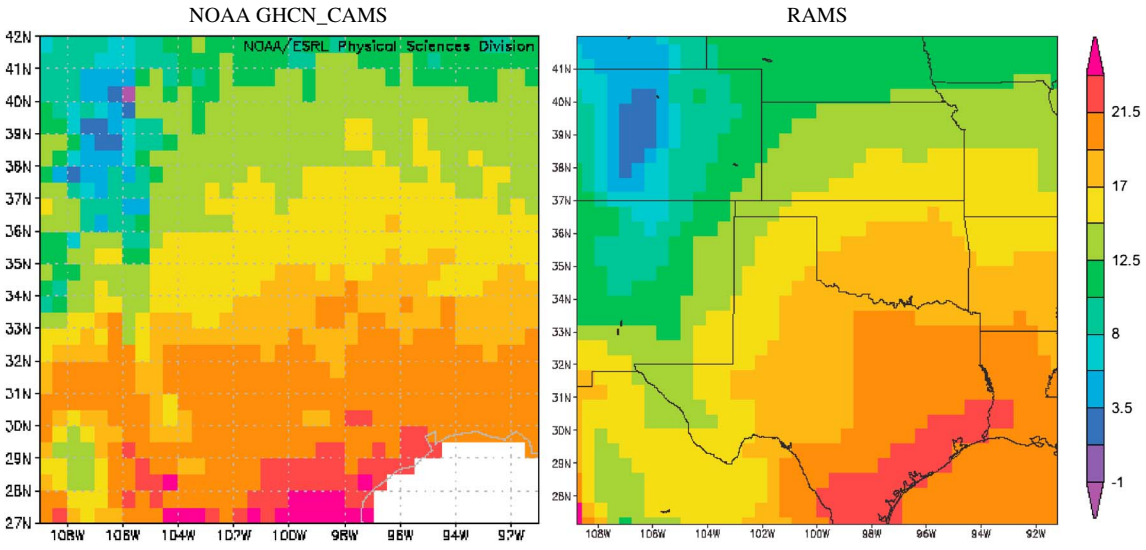

Figure 4. Comparison of averaged surface air temperature (screen height, °C) from observation (NOAA GHCN_CAMS) and that from RAMS in the year 2003.

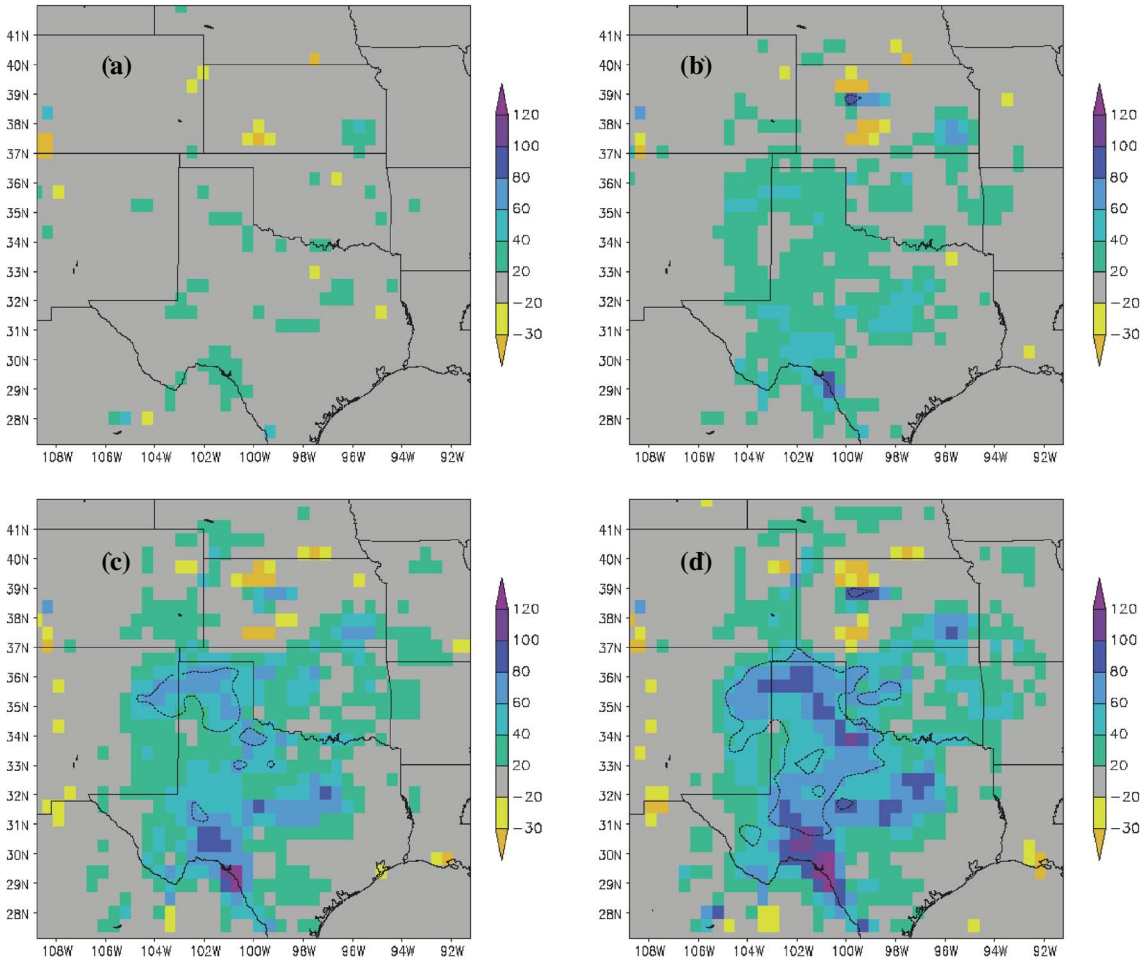

Figure 5. Differences of accumulated precipitation (mm) between simulation without woody encroachment and simulations with (a) 10% encroachment (R10 – R0), (b) 40% encroachment (R40 – R0), (c) 70% encroachment (R70 – R0), and (d) 100% encroachment (R100 – R0). Dotted contour lines in Figures 5b, 5c, and 5d indicate 95% confidence level from Student's *t* test.

representing the magnitude of woody plant expansion at the regional scale, which is the primary concern of this study. It would be ideal to have a time series of maps based on historically observed woody plant encroachment. This kind of time series does not exist at the regional scale. Also, it is difficult to realistically predict future changes in landscape including the composition of grasses and woody plants.

[13] The derived woody plant expansion is then inserted in the climate model. In the RAMS model, the built-in AVHRR land cover data set is in 1 km resolution. In this study, woody encroachment maps such as those in Figure 2 are used to replace the built-in land cover data by using correct spatial dimension and file format (binary) and modifying source code. One kilometer land cover pixels are then grouped into a number of patches (10 in this study) in each 50 × 50 km grid cell. There are a total of 11 land cover maps representing different degrees of woody encroachment (0%, 10%, 20%, 30%, 40%, 50%, 60%, 70%, 80%, 90%, and 100%). As a result, there are 11 runs of the climate model. The purpose of gradually invading grassland and having a set of climate simulations is to investigate if there is a threshold in woody cover percentage that would affect regional climate. It was initially hypothesized that the impacts are insignificant when woody encroachment is low, but the impacts would be significantly increased when woody encroachment reaches a threshold (e.g., 50%).

2.4. Woody Encroachment and Biophysical Changes

[14] Effects of vegetation change on climate are results of changes in surface biophysical characteristics, which can directly affect fluxes of mass and energy between ecosystems and the atmosphere. Table 1 lists major biophysical variables that have been under extensive study in land/climate interactions. All five of these variables are crucial surface parameters used in LEAF-2 model in RAMS. Vegetation may also affect the climate by biogeochemical processes, which are not a focus of this study.

[15] Woody plant encroachment into grassland changes every biophysical parameter listed in Table 1. Red cedar, like many woody plants, is evergreen and has a high leaf area index resulting in relatively high percentages of precipitation interception [*Wilcox*, 2002]. Woody vegetation, by virtue of being more deeply rooted, generally extracts soil water from greater depths than does herbaceous vegetation. Higher leaf area index and greater rooting depth increase surface evapotranspiration and thus can lead to surface cooling and

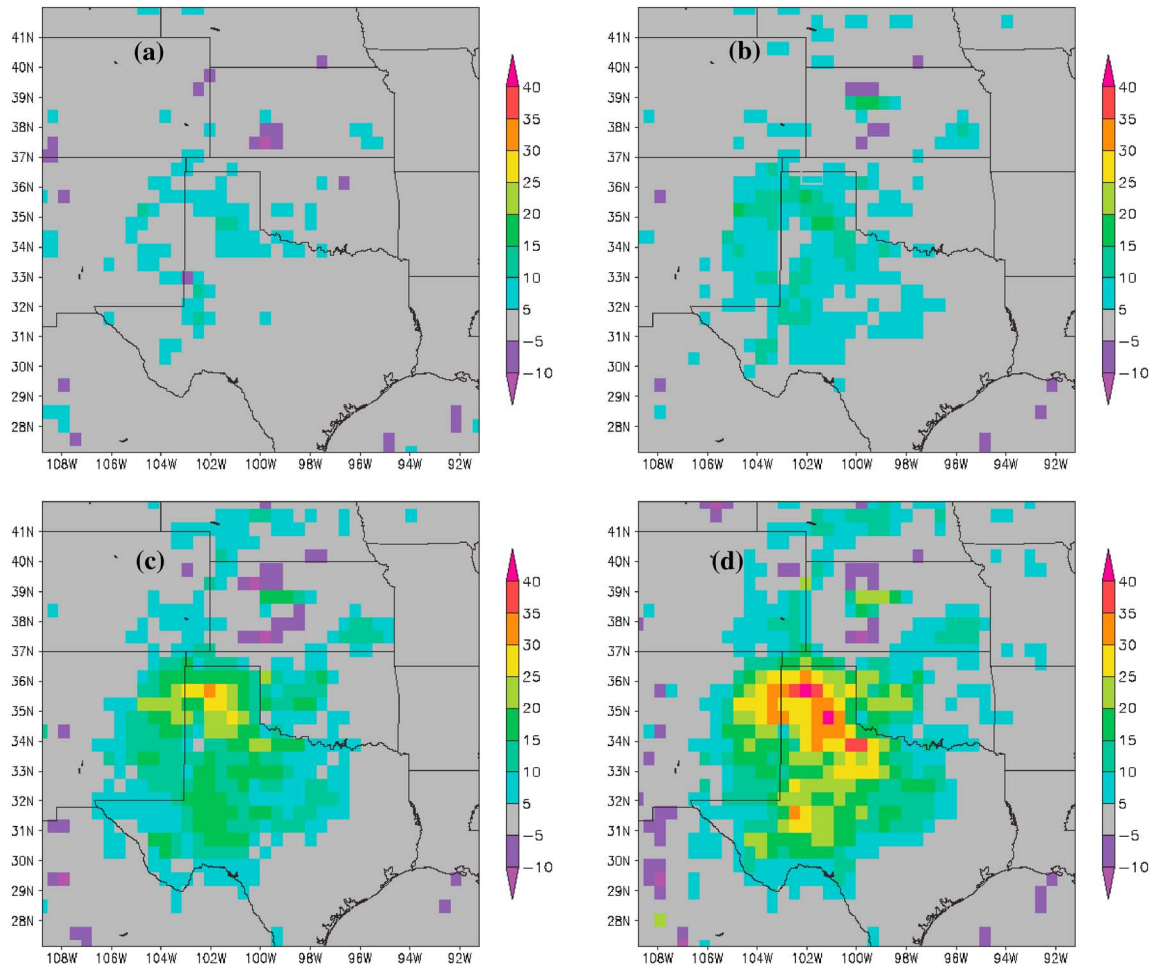

Figure 6. Precipitation increases in percentage: (a) 10% encroachment (R10/R0 × 100), (b) 40% encroachment (R40/R0 × 100), (c) 70% encroachment (R70/R0 × 100), and (d) 100% encroachment (R100/R0 × 100).

increased precipitation. However, the moisture for evapotranspiration is relatively limited in semiarid regions like the southern Great Plains. On the other hand, replacing grassland by woody species can result in a higher percentage of bare soil and thus lower fractional vegetation cover, and therefore would tend to increase surface temperature. This, together with higher roughness of woody plants and fragmented surface characteristics, further promotes the flux of moisture to the atmosphere through enhanced turbulence. More importantly, evergreen woody plants tend to have lower surface albedo (they are darker), particularly in the winter when herbaceous vegetation turns senescent. The photograph in Figure 1 (right) shows red cedar-encroached grassland in winter, and the contrast in albedo is striking. As a result of changes in surface biophysical characteristics and related changes in mass and energy fluxes, it is very likely that woody plant encroachment may modify local to regional climate, but it is unknown which processes dominate and what the overall direction of change will be over a particular region like the southern Great Plains.

[16] Table 2 lists biophysical parameters for shortgrass and wooded grassland that are used in RAMS. In this study, woody plant encroachment is treated simply as wooded grassland replacing shortgrass. If there are any impacts resulting from woody encroachment, it is ultimately due to changes in these biophysical parameters. In Table 2, albedo, leaf area index, and roughness length have substantial differences between shortgrass and wooded grassland, while differences of fractional vegetation cover and root depth are minimal. Seasonal changes of these parameters are represented by simple mathematical functions that are dependent on latitude and day of the year. In this study, the built-in biophysical parameters in RAMS in Table 2 are used and no attempt is made to validate these parameters. In Table 2, rooting depth and fractional cover are the same for shortgrass and wooded grassland. In reality they may be different. For example, woody vegetation is generally more deeply rooted as discussed in the previous text.

[17] In this study, there are a total of 11 RAMS runs each with a different amount of woody encroachment (0%, 10%, 20%, 30%, 40%, 50%, 60%, 70%, 80%, 90%, and 100%). Changes in precipitation and temperature are examined among this set of RAMS simulations to determine the impacts of woody plant encroachment on climate. Additionally, trends of simulated precipitation and temperature are examined to look at how climate system responds to this gradual land surface change and to identify if there is a threshold of impacts.

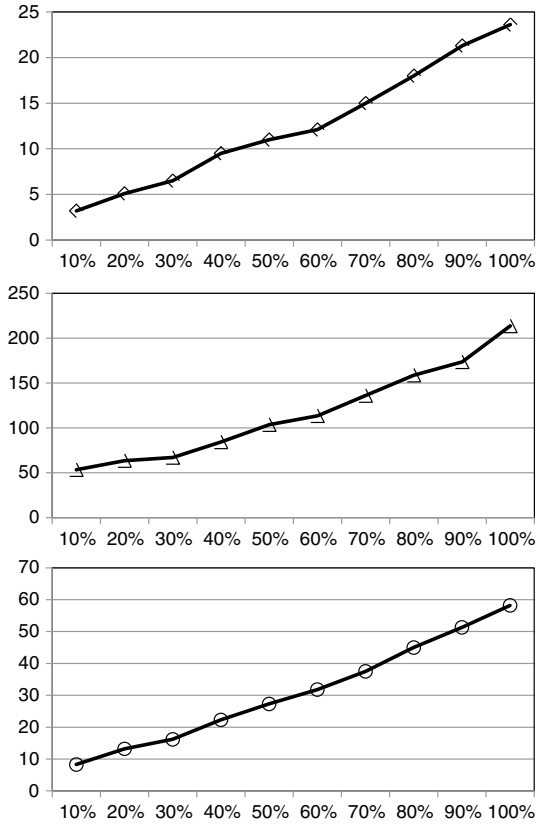

Figure 7. Precipitation increase (mm) in response to a range of woody encroachment (0%–100%). (top) Domain average of total annual precipitation; (middle) domain maximum of total annual precipitation; (bottom) average of total annual precipitation over a focus area (latitude 29°N–37.5°N, longitude 104.7°W–95.7°W).

3. Results

[18] The performance of RAMS was first assessed by comparing the RAMS-simulated precipitation and screen height air temperature for 2003 against observed data. In this study, the precipitation data use retrievals from the Tropical Rainfall Measuring Mission (TRMM) satellite. TRMM is a joint satellite between NASA and the Japan Aerospace Exploration Agency, launched in November 1997 [*Simpson et al*., 1988]. Its primary mission is to measure precipitation in the tropics, using both active and passive microwave instruments. This study uses TRMM 3B42 version 6 data products which have 3 h temporal resolution and $0.25° \times 0.25°$ spatial resolution. Data plots can be generated directly online at http://disc2.nascom.nasa.gov/Giovanni/tovas/. The screen height air temperature data use the Global Historical Climatology Network and Climate Anomaly Monitoring System (GHCN_CAMS) data from NOAA [*Fan and van den Dool*, 2008]. GHCN_CAMS is a high-resolution (0.5°) global land surface temperature data set from 1949 to present.

[19] Figure 3 shows TRMM-observed rainfall and RAMS-simulated rainfall in 2003. Overall, RAMS captures the rainfall pattern well. In this time period, rainfall concentrates over the south and the east portion of the study area. Over the central, the western, and the northern part, rainfall is scarce with the maximum not exceeding 400 mm. This low rainfall area in New Mexico, northern Texas, western Oklahoma and Kansas, and nearby area corresponds to arid to semiarid climate conditions in this region. However, high rainfall (>1200 mm) observed by TRMM is over the southeast corner of the domain including the Gulf of Mexico, Louisiana, and southeastern Texas. RAMS-simulated high rainfall occurs over the east of the domain and a smaller area in the south. Rain over the Gulf of Mexico is very limited. In this study, no attempt is made to "tune" RAMS in simulating precipitation. Additionally, RAMS' grid increment (50 km) is much lower than TRMM's (about 27 km).

[20] Figure 4 shows observed 2 m air temperature from NOAA GHCN_CAMS data and RAMS-simulated 2 m air temperature averaged in 2003. GHCN_CAMS only covers land surface and thus does not have data over the Gulf of Mexico. Two meter air temperature in RAMS is extracted using the RAMS/HYPACT Evaluation and Visualization Utilities which is the package for generating graphic representations and reformatting RAMS model output. GHCN_CAMS' 0.5° grid increment is very close to RAMS' 50 km grid spacing. Figure 4 shows that RAMS performs better in simulating air temperature than precipitation. High temperature near the Gulf of Mexico, temperature gradient from south to north, and low temperature over the Rocky Mountain are very well captured. However, the northern part of the domain is generally cooler than observation, and RAMS is not able to simulate some localized temperature variation.

[21] This study finds that woody plant encroachment tends to increase precipitation. Figure 7 shows precipitation differences between the simulation without encroachment and simulations with encroachment. For the convenience of discussion, let R0, R10, R20 … R90, R100 denote 11 RAMS runs. Figure 7 shows precipitation impacts from four selected encroachment scenarios: $R10 - R0$, $R40 - R0$, $R70 - R0$, and $R100 - R0$. Over some scattered areas, precipitation decreases slightly in response to woody encroachment which is shown in Figure 2. In general, however, precipitation increases gradually as encroachment increases. With 10% encroachment, precipitation increase is scattered and less than 40 mm. With 40% encroachment, precipitation increase becomes greater (>40 mm) and more concentrated in Texas and surrounding areas. With 70% encroachment, more areas have >40 mm precipitation increase and some areas begin to have >100 mm increase. When encroachment reaches 100%, precipitation increases dramatically with large areas experiencing >80 mm increase. Spatially, precipitation change generally corresponds to where encroachment occurs (Figure 2). A large part of Texas, eastern New Mexico, and western Oklahoma has the greatest change in precipitation. Dotted contour lines in Figure 5 represent statistically significant increase in precipitation at 95% confidence level. Student's *t* test is conducted between a pair of simulations (e.g., R100 and R0) based on a time series of precipitation rates at each grid cell. Areas with statistically significant increase in precipitation are more pronounced in areas with more encroachment and are primarily located in northern Texas, eastern New Mexico, and western Oklahoma.

[22] The same amount of increase in precipitation can have different meanings to different areas. Figure 6 shows precipitation increases in percentage. As in Figure 5,

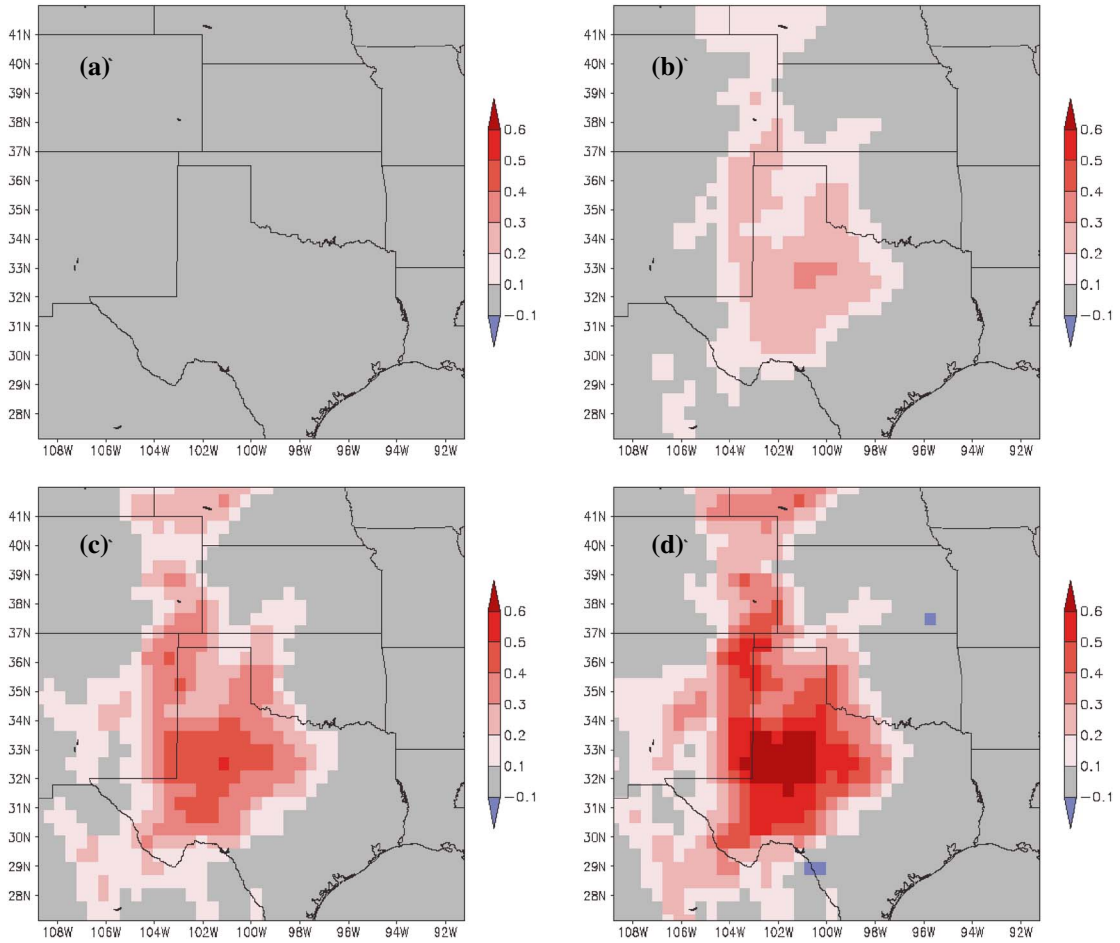

Figure 8. Differences of maximum air temperature (2100 UTC, °C) between simulation without woody encroachment and simulations with (a) 10% encroachment (R10 − R0), (b) 40% encroachment (R40 − R0), (c) 70% encroachment (R70 − R0), and (d) 100% encroachment (R100 − R0). None is statistically significant at 95% confidence level.

precipitation increases gradually as encroachment spreads and spatially the increase approximately follows encroachment. However, the largest increase in percentage becomes to concentrate in northern Texas and nearby. Some wet areas (e.g., southern Texas) where precipitation increases substantially (>100 mm) do not have a large percentage increase. In contrast, dry areas (e.g., northern Texas, western Oklahoma, and eastern New Mexico) have the largest increase in percentage even though the amount of increase is moderate. In northern Texas, a large area has precipitation increase of over 30% when woody encroachment is 100%. This change is substantial for this dry area.

[23] Figure 7 presents three graphs that illustrate how precipitation responds to a range of woody encroachment from 0% to 100% on the surface. Figure 7 (top) shows precipitation increase averaged over the entire domain, Figure 7 (middle) shows maximum change in the domain, and Figure 7 (bottom) focuses on a smaller area which is approximately defined between 29°N–37.5°N in latitude and 104.7°W–95.7°W in longitude. This focus area is roughly in central and northern Texas and corresponds to the greatest encroachment and precipitation change. These graphs are used to detect if there is any apparent trend in precipitation change (e.g., precipitation increase levels off at a certain amount of encroachment). All these three graphs indicate that precipitation increases almost linearly in response to increasing encroachment. Averaged over the entire domain, precipitation increases by 3.2 mm at 10% encroachment and reaches 23.6 mm at 100% encroachment. The maximum increase is 53.4 mm at 10% encroachment and 213.58 mm at 100% encroachment. In the focus area, average increase is 8.3 mm at 10% encroachment and reaches 58.2 mm at 100% encroachment. From these graphs, it appears that the rate of precipitation change remains almost constant. There is no apparent tipping point where the rate increases significantly nor a leveling-off point where the rate suddenly decreases at certain encroachment.

[24] Screen height air temperature simulated by RAMS at different encroachment is also analyzed. Both maximum and minimum daily air temperatures (21:00 UTC and 09:00 UTC) are examined. Figure 8 shows differences of maximum daily temperature between the simulation without encroachment and simulations with encroachment. It is similar to Figure 5, but the variable is now air temperature. Student's t test is also conducted, but no area is found to have statistically significant increase (95% confidence level) in temperature even with 100% encroachment. Overall, woody encroachment leads to a strong warming effect

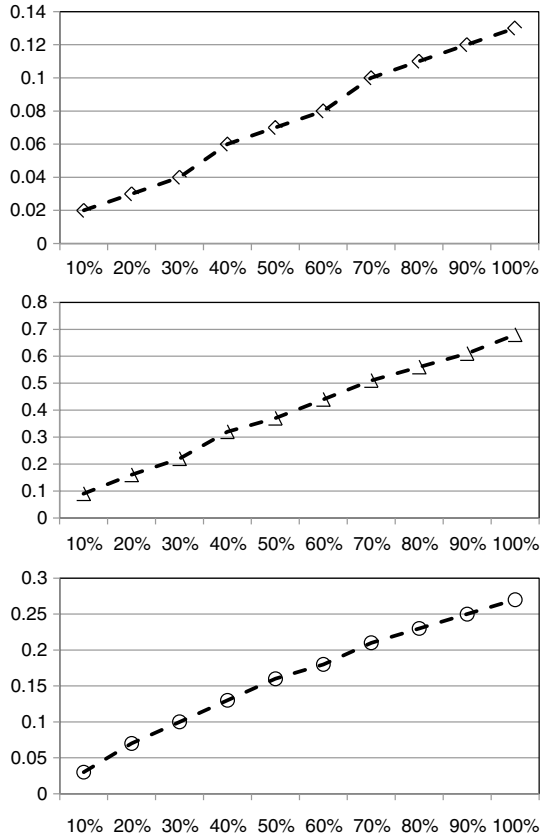

Figure 9. Maximum air temperature increase (°C) in response to a range of woody encroachment (0%–100%). (top) Domain average of annual mean difference; (middle) domain maximum of annual mean difference; (bottom) average of annual mean difference over a focus area (latitude 29°N–37.5°N, longitude 104.7°W–95.7°W).

during the day in this area. At 10% encroachment, temperature does not change much. With 40% encroachment, air temperature increases by 0.1°C to 0.3°C in a large area of northern Texas. With 70% encroachment, more areas begin to experience higher temperature and the change is as high as 0.4°C in certain places. When encroachment reaches 100%, a large part of central to northern Texas has an increase of 0.3°C to 0.6°C. Temperature in eastern Colorado and western Nebraska increases by 0.2°C to 0.4° C. Spatially, the warming effects follow more closely to woody encroachment on the surface than changes in precipitation. However, an area in southern Texas and near the U.S.-Mexico border has substantial woody encroachment on the surface (Figure 2) but does not have noticeable change in temperature. This area has high simulated rainfall which may have dampened the warming effects.

[25] Similar to precipitation, Figure 9 shows changes in maximum air temperature over a range of 0% to 100% encroachment on the surface. Figure 9 (top) shows temperature change averaged over the entire domain and over the 1 year period. Figure 9 (middle) shows maximum change in the domain. Figure 9 (bottom) focuses on a smaller area which is approximately defined between 29°N–37.5°N in latitude and 104.7°W–95.7°W in longitude, and this focus area corresponds to the greatest encroachment and precipitation change. Figure 9 shows that temperature increases almost linearly with increasing woody encroachment. There is no abrupt change in the warming trend. Averaged over the entire domain, temperature increases by 0.02°C at 10% encroachment and reaches 0.13°C at 100% encroachment. Spatially, the maximum increase at a grid point is 0.09°C at 10% encroachment and 0.68°C at 100% encroachment. In the focus area, average temperature increase is 0.03°C at 10% encroachment and becomes 0.27°C at 100% encroachment.

[26] Figure 10 shows how maximum temperature during the day changes over the year as a result of woody encroachment and also how this temporal dynamic relates to rainfall events. Figure 10 (top) shows the temperature difference (R100 – R0) averaged over the domain in the 12 month period. Figure 10 (bottom) shows daily precipitation. It appears that how temperature changes in response to woody encroachment is affected by rain. When there is little rain, for example, in July and December, the warming effect of encroachment is apparent. When there is rain, however, woody encroachment tends to have a cooling effect. High rainfall in September corresponds to strong cooling. Rainfall in February, March, June, early October, mid-November, and other periods decreases surface warming. The correlation coefficient between temperature change (Figure 10, top) and precipitation rate (Figure 10, bottom)

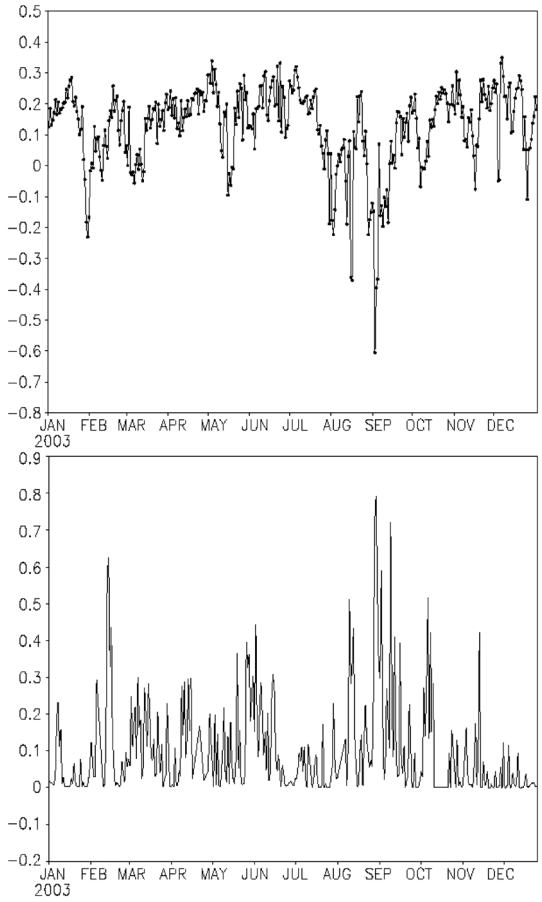

Figure 10. (top) Time series of domain averaged difference of maximum air temperature (R100 – R0) versus (bottom) time series of precipitation rate.

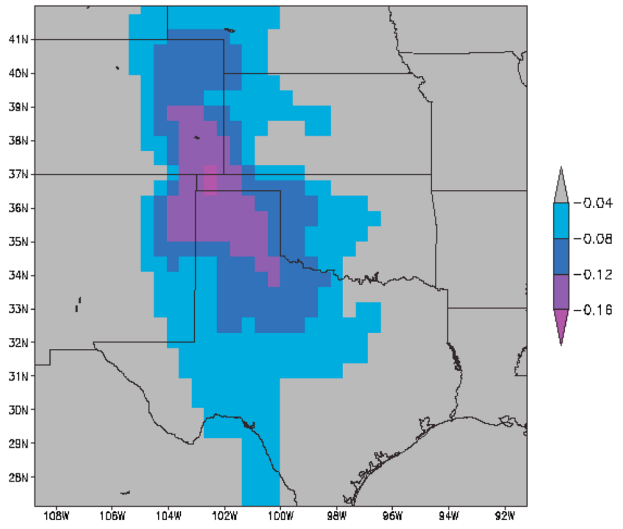

Figure 11. Differences of minimum air temperature (0900 UTC, °C) between simulation without woody encroachment and simulation with 100% encroachment (R100 – R0).

is −0.52. This explains the earlier finding in the previous text that surface warming (Figure 8) tends to be in the dry area and away from the rain belt (Figure 3). During some time periods, however, the relationship between rainfall and surface cooling is not well defined. For example, a strong cooling occurs in late January. There is not much rain at the same time and high rainfall occurs a few weeks later in mid-February. This particular relationship between temperature change and rain may be due to the fact that rain does not always fall over the encroached area and also soil moisture is uniformly specified at the beginning of each run.

[27] Figure 11 shows the impact of woody encroachment on minimum air temperature at screen height (R100 – R0). Compared to maximum air temperature during the day, minimum temperature (09:00 UTC) is less affected. There is a slight cooling effect in the encroached areas, but the decrease is lower than 0.16°C even with 100% encroachment. Averaged over the entire domain, the minimum temperature drops by 0.03°C with 100% encroachment.

4. Discussions

[28] Results presented previously show that woody encroachment has strong impacts on precipitation and daytime air temperature in this region. Discussions here try to explain why precipitation and temperature respond to woody encroachment in this particular way.

[29] As discussed at the beginning, woody encroachment modifies key biophysical variables on the surface including albedo, leaf area index (LAI), fractional vegetation cover, rooting depth, and surface roughness. Table 2 shows that woody encroachment leads to lower albedo, higher LAI, and higher surface roughness in RAMS. Changes in these biophysical variables alter energy fluxes between the surface and the overlying atmosphere, which in turn influence precipitation and temperature. Lower albedo (0.26 to 0.18) increases net radiation which may result in higher sensible and latent heat flux. Higher LAI (2.0 to 5.0) tends to increase evapotranspiration and thus latent heat flux when moisture is not limited. Higher surface roughness at the same time promotes vertical motion and turbulent fluxes. All these variables have played a role in simulated impacts from woody encroachment.

[30] Figure 12 shows decreased albedo when shortgrass is completely replaced by woody species (R100 – R0). Albedo change corresponds well with woody encroachment distribution in Figure 2. The largest decrease takes place in central and northern Texas and nearby areas. Figure 13 shows changes in surface sensible and latent heat fluxes at 100% encroachment (R100 – R0). Both sensible (Figure 13, top) and latent (Figure 13, bottom) fluxes have increased, and the overall pattern is similar to that seen in the woody encroachment map and changes in albedo. However, while sensible heat flux increases as much as 50 W/m^2 and more in a large part of central to northern Texas, increase in latent heat flux is generally much smaller (<20 W/m^2). Only over a small area in southern Texas where RAMS-simulated rainfall is high (Figure 3), latent heat flux has increased up to 50 W/m^2. This indicates that changes in albedo have more impacts on surface fluxes and thus climate variables than LAI does where moisture is limited. As a result of this, the warming effect from decreased albedo is much greater than the cooling effect from increased vegetation and evapotranspiration. This further explains observations in Figure 10 in which the warming effect is more pronounced when rain and soil moisture are limited.

[31] Figure 14 shows changes in low-level vertical velocity at 100% encroachment. It is a 12 month average of all vertical cross sections in the x-z plane over the latitude belt from 29°N to 37.5°N. Changes in precipitation approximately take place over this latitude belt. Figure 14 shows that vertical velocity increases greatly between longitudes 105°W and 100°W and decreases slightly in the east. Vertical motions can lead to variations in mesoscale convective rainfall. It is not surprising that the surface area defined by 29°N to 37.5°N in latitude and 105°W and 100°W in longitude is located in the central and northern Texas where most of the increases of precipitation

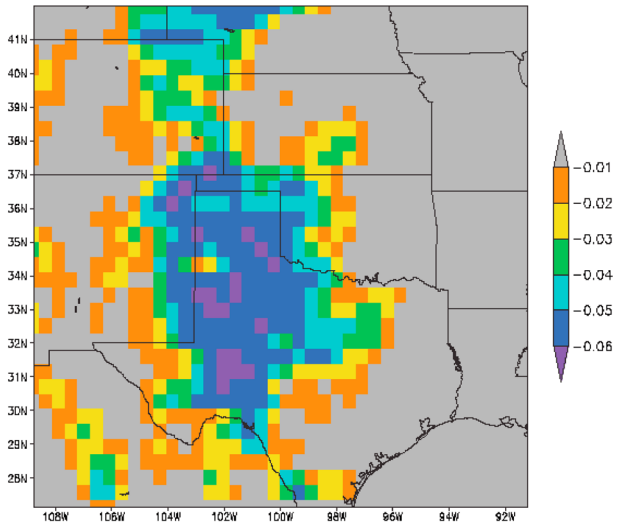

Figure 12. Albedo decrease at 100% encroachment.

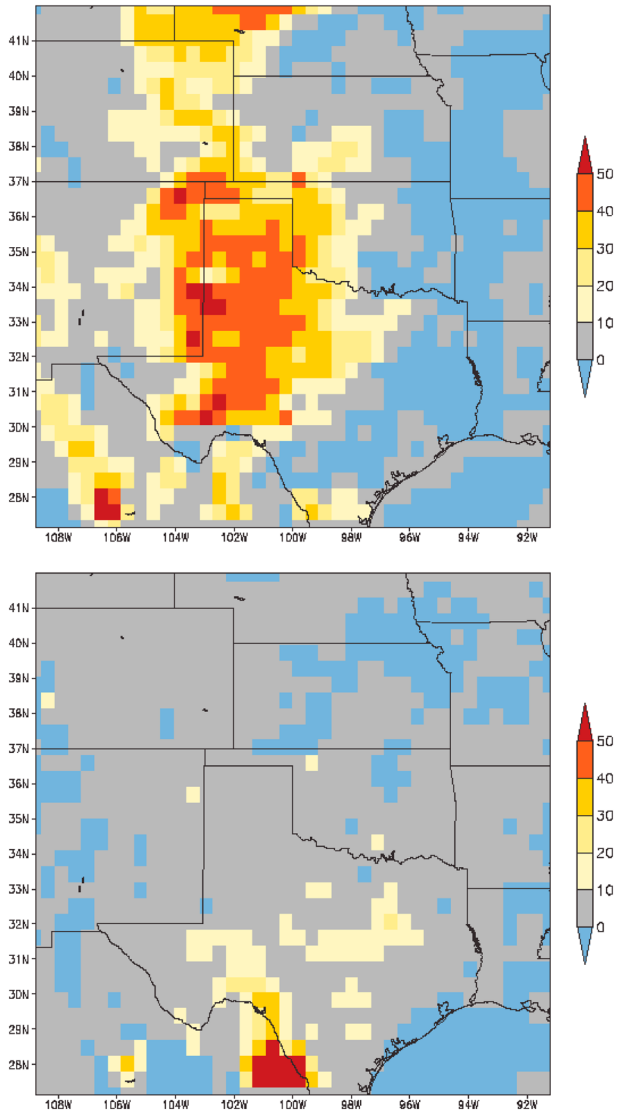

Figure 13. Changes in (top) sensible heat flux (W/m^2) and (bottom) latent heat flux (W/m^2) at 100% encroachment. Both sensible and latent heat fluxes are 1 year average at 2100 UTC.

take place. Stronger surface heating due to decreased albedo and thus increased sensible heat flux together with greater surface roughness may have caused this increase in vertical motion. To a lesser degree, increased surface LAI and evapotranspiration may have contributed more moisture when it is available.

[32] A few factors need to be considered to further improve this study. First, the actual decrease in albedo, as well as increase in LAI, needs to be verified using observation data, possibly from satellite. The albedo value (0.26 for shortgrass and 0.18 for wooded grassland) is built in the RAMS model and may not be suitable for this region. The albedo values need to be validated using observational data. This also applies to other biophysical variables listed in Table 2 such as root depth. Second, the method to generate the spread of woody species is not perfect. As stated earlier, woody encroachment does not take place randomly over the space. One solution to this is to use satellite data to observe how exactly woody encroachment has been occurring in the past and then use this information to project into the future. Lastly, the impacts of RAMS model configuration need to be thoroughly examined. Horizontal grid spacing, convection schemes, and accuracy of simulated soil moisture may influence the effects observed in this study. Follow-on studies are necessary to further investigate the impacts of these factors.

5. Summary

[33] Across arid and semiarid ecosystems around the world, conversion of grassland to woodland is widespread. This study focuses on the southern Great Plains of the U.S. and uses a regional model to simulate the effects of this phenomenon on regional climate system. Grassland is invaded gradually in the model, and model-simulated precipitation and air temperature are examined. This study finds that woody encroachment leads to a statistically significant increase in rainfall in this region and it also has an overall warming effect, but the change in temperature is not statistically significant. More encroachment on the surface leads to stronger warming and more rainfall, and the relationship between the amount of encroachment and increase in temperature and precipitation is almost linear. Spatially, the strongest impacts on climate are found in the dry areas and are consistent with locations of encroachment. Decreased albedo as a result of encroachment appears to be the most important biophysical change that causes changes in climate. Because of limited moisture in a large part of the encroached areas, lower albedo leads to a strong increase in sensible heat flux and warming in the air. Heating on the surface further promotes vertical motion of air, which in turn brings more convective rainfall.

[34] This study demonstrates the importance of land cover changes in climate system. In the future, climate modeling, particularly studies at regional scales, needs to incorporate such large-scale surface disturbances. The use of satellite-observed surface changes and more accurate biophysical parameters to improve surface representation may become more and more necessary to achieve such purposes.

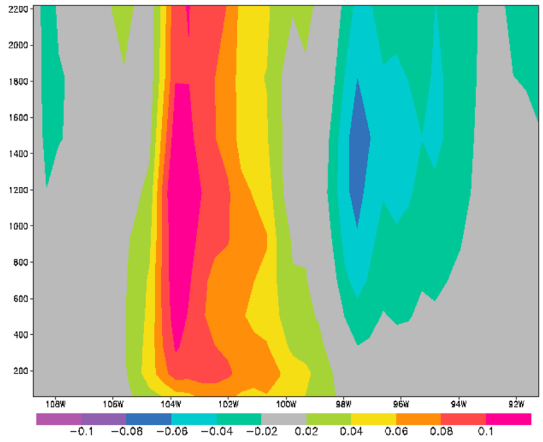

Figure 14. Difference (R100 − R0) in vertical velocity (cm/s) averaged between 29°N and 37.5°N in latitude. The difference is 1 year average at 2100 UTC.

References

Anav, A., P. M. Ruti, V. Artale, and R. Valentini (2010), Modelling the effects of land-cover changes on surface climate in the Mediterranean region, *Clim. Res.*, *41*, 91–104.

Archer, S. (1994), Woody plant encroachment into southwestern grasslands and savannas: Rates, patterns and proximate causes, in *Ecological Implications of Livestock Herbivory in the West*, edited by M. Vavra, W. A. Laycock, and R. D. Pieper, 13–68, Society for Range Management, Denver.

Archer, S. (2002), Proliferation of woody plants in grasslands and savannas: A bibliography, University of Arizona, http://ag.arizona.edu/research/archer/research/biblio1.html.

Archer, S., D. S. Schimel, and E. A. Holland (1995), Mechanisms of shrubland expansion: Land use, climate or CO_2?, *Clim. Change*, *29*, 91–99.

Betts, R. A. (2000), Offset of the potential carbon sink from boreal forestation by decreases in surface albedo, *Nature*, *408*, 187–190.

Betts, R. A. (2006), Forcings and feedbacks by land ecosystem changes on climate change, *J. Phys. IV Fr.*, *139*, 119–142.

Bonan, G. B., D. Pollard, and S. L. Thompson (1992), Effects of boreal forest vegetation on global climate, *Nature*, *359*, 716–718.

Briggs, J. M., G. A. Hoch, and L. C. Johnson (2002), Assessing the rate, mechanisms, and consequences of the conversion of tallgrass prairie to *Juniperus virginiana* forest, *Ecosystems*, *5*, 578–586.

Coppedge, B. R., D. M. Engle, R. E. Masters, and M. S. Gregory (2004), Predicting juniper encroachment and CRP effects on avian community dynamics in southern mixed-grass prairie, *U.S.A. Biol. Conserv.*, *115*, 431–441.

Cotton, W. R., and R. A. Pielke Sr. (2007), *Human Impacts on Weather and Climate*, 2nd ed., Cambridge University Press, New York.

Cotton, W. R., et al. (2003), RAMS 2001: Current status and future directions, *Meteorol. Atmos. Phys.*, *82*, 5–29.

Defries, R. S., and J. R. G. Townshend (1995), NDVI-derived land cover classification at a global scale, *Int. J. Remote Sens.*, *15*, 3567–3586.

Engle, D. M., B. R. Coppedge, and S. D. Fuhlendorf (2007), From the dust bowl to the Great Green Glacier: Human activity and environmental change in Great Plains grasslands, In Van Auken, OW (Ed.) Western North American *Juniperus* Communities—A Dynamic Vegetation Type, Springer.

Fall, S., D. Niyogi, A. Gluhovsky, R. A. Pielke Sr., E. Kalnay, and G. Rochon (2009), Impacts of land use land cover on temperature trends over the continental United States: Assessment using the North American Regional Reanalysis, *Int. J. Climatol.*, doi:10.1002/joc.1996.

Fan, Y., and H. van den Dool (2008), A global monthly land surface air temperature analysis for 1948-present, *J. Geophys. Res.*, *113*, D01103, doi:10.1029/2007JD008470.

Feddema, J. J., K. W. Oleson, G. B. Bonan, L. O. Mearns, L. E. Buja, G. A. Meehl, and W. M. Washington (2005), The importance of landcover change in simulating future climates, *Science*, *310*, 1674–1678.

Foley, J. A., M. H. Costa, C. Delire, N. Ramankutty, and P. Snyder (2003), Green surprise? How terrestrial ecosystems could affect Earth's climate, *Front. Ecol. Environ.*, *1*, 38–44.

Forster, P., et al. (2007), Changes in atmospheric constituents and in radiative forcing, in *Climate Change 2007: The Physical Science Basis. Contribution of Working Group I to the Fourth Assessment Report of the Intergovernmental Panel on Climate Change*, edited by S. Solomon, D. Qin, M. Manning, Z. Chen, M. Marquis, K. B. Averyt, M. Tignor, and H. L. Miller, pp. 129–234, Cambridge University Press, Cambridge, UK and New York, USA.

Fuhlendorf, S. D. (1999), Ecological considerations for woody plant management, *Rangelands*, *21*, 12–15.

Fuhlendorf, S. D., S. R. Archer, F. E. Smeins, D. M. Engle, and C. A. Jr.Taylor (2008), The combined influence of grazing, fire, and herbaceous productivity on tree-grass interactions, in *Western North American Juniperus Communities*, p. 219–238, edited by O. Van Auken, Springer, New York.

Gao, X. J., Y. Luo, W. T. Lin, Y. Luo, W. T. Lin, Z. C. Zhao, and F. Giorgi (2003), Simulation of effects of landuse change on climate in China by a regional climate model, *Adv. Atmos. Sci.*, *20*(4), 583–592.

Ge, J., J. Qi, B. Lofgren, N. Moore, N. Torbick, and J. M. Olson (2007), Impacts of land use/cover classification accuracy on regional climate simulations, *J. Geophys. Res.*, *112*, D05107, doi:10.1029/2006JD007404.

Ge, J., J. Qi, and B. Lofgren (2008), Use of vegetation properties from EOS observations for land-climate modeling in East Africa, *J. Geophys. Res.*, *113*, D15101, doi:10.1029/2007JD009628.

Giorgi, F., and L. O. Mearns (1999), Introduction to special section: Regional climate modeling revisited, *J. Geophys. Res.*, *104*, 6335–6352, doi:10.1029/98JD02072.

Huxman, T. E., B. P. Wilcox, and D. D. Breshears (2005), Ecohydrological implications of woody plant encroachment, *Ecology*, *86*, 308–319.

Jacob, D., and R. Podzun (1997), Sensitivity studies with the regional climate model REMO, *Meteorol. Atmos. Phys.*, *63*, 119–129, doi:10.1007/BF01025368.

Kalnay, E., et al. (1996), The NCEP/NCAR 40-year reanalysis project, *Bull. Am. Meteorol. Soc.*, *77*, 437–471.

Lee, T. J. (1992), The impact of vegetation on the atmospheric boundary layer and convective storms, *Atmos. Sci. Pap.*, 509, Colorado State University, Fort Collins, Colo.

Loveland, T. R., B. C. Reed, J. F. Brown, D. O. Ohlen, Z. Zhu, L. Yang, and J. W. Merchant (2000), Development of a global land cover characteristics database and IGBP DISCover from 1 km AVHRR data, *Int. J. Remote Sens.*, *21*, 1303–1330.

Miller, R. F., and J. A. Rose (1995), Historic expansion of *Juniperus occidentalis* (western juniper) in southeastern Oregon, *G. Basin Nat.*, *55*(1), 37–45.

Nair, U. S., D. K. Ray, J. Wang, S. A. Christopher, T. J. Lyons, R. M. Welch, and R. A. Pielke, Sr. (2007), Observational estimates of radiative forcing due to land use change in southwest Australia, *J. Geophys. Res.*, *112*, D09117, doi:10.1029/2006JD007505.

de Noblet-Ducoudré, et al. (2011), Determining robust impacts of land-use-induced land-cover changes on surface climate over North America and Eurasia: Results from the first set of LUCID experiments, *J Clim.*, *25*, 3261–3281.

Pielke, R. A., Sr., et al. (1992), A comprehensive meteorological modeling system—RAMS, *Meteorol. Atmos. Phys.*, *49*, 69–91.

Pielke, R. A., Sr., J. Adegoke, A. Beltran-Przekurat, C. A. Hiemstra, J. Lin, U. S. Nair, D. Niyogi, and T. E. Nobis (2007), An overview of regional land-use and land-cover impacts on rainfall, *Tellus*, *59B*, 587–601.

Pielke, R. A., Sr., et al. (2011), Land use/land cover changes and climate: Modeling analysis and observational evidence, *WIREs Clim Change*, *2*, 828–850, doi:10.1002/wcc.144.

Pitman, A. J., G. T. Narisma, R. A. Pielke, Sr., and N. J. Holbrook (2004), The impact of land cover change on the climate of southwest western Australia, *J. Geophys. Res.*, *109*, D18109, doi:10.1029/2003JD004347.

Schmidt, T. L., and E. C. Leatherberry (1995), Expansion of eastern redcedar in the lower Midwest, *Northern J. Appl. For.*, *12*, 180–183.

Scott, R. L., T. E. Huxman, D. G. Williams, and D. C. Goodrich (2006), Ecohydrologicla impacts of woody-plant encroachment: Seasonal patterns of water and carbon dioxide exchange within a semiarid riparian environment, *Global Change Biol.*, *12*, 311–324.

Shukla, J., C. Nobre, and P. Sellers (1990), Amazon deforestation and climate change, *Science*, *247*, 1322–1325.

Simpson, J., R. F. Adler, and G. R. North (1988), A proposed Tropical Rainfall Measuring Mission (TRMM) satellite, *Bull. Am. Meteorol. Soc.*, *69*, 278–295.

Taylor, C. A. (2005), Prescribed burning cooperatives: Empowering and equipping ranchers to manage rangelands, *Rangelands*, *27*, 18–22.

Tremback, C. J., and R. Kessler (1985), A surface temperature and moisture parameterization for use in mesoscale models, in *Seventh Conf. on Numerical Weather Prediction*, pp. 355–358, *Amer. Meteor. Soc.*, Montreal, Canada.

Walko, R. L., et al. (2000), Coupled atmosphere-biophysics-hydrology models for environmental modeling, *J. Appl. Meteorol.*, *39*, 931–944.

Wilcox, B. (2002), Shrub control and streamflow on rangelands: A process based viewpoint, *J. Range Manage.*, *55*, 318–326.